AJNR

This information is current as of May 9, 2025.

MR Imaging in the Management of Supratentorial Intracranial AVMs

H. J. Smith, C. M. Strother, Y. Kikuchi, T. Duff, L. Ramirez, A. Merless and S. Toutant

AJNR Am J Neuroradiol 1988, 9 (2) 225-235
http://www.ajnr.org/content/9/2/225

MR Imaging in the Management of Supratentorial Intracranial AVMs

H. J. Smith[1, 2]
C. M. Strother[1]
Y. Kikuchi[1]
T. Duff[3]
L. Ramirez[3]
A. Merless[4]
S. Toutant[5]

The MR images, CT scans, and angiograms of 15 consecutive patients with intracranial, supratentorial arteriovenous malformations (AVMs) were studied retrospectively. The three imaging techniques were evaluated separately to assess their utility in defining the size, characteristics, and location of the AVM nidus, its arterial supply, and venous drainage. The studies were also evaluated for their ability to show associated parenchymal abnormalities, the presence of mass effect, and changes occurring after embolization.

MR was superior to both CT and angiography in showing the exact anatomic relationships of the nidus, feeding arteries, and draining veins, as well as in demonstrating the extent of AVM nidus obliteration after embolization. MR was more sensitive than CT in revealing associated parenchymal abnormalities and subacute hemorrhage. Because of flow-related artifacts and low sensitivity in distinguishing calcification from rapid flow and/or hemosiderin, MR seemed to have a low sensitivity for detecting old hemorrhage within an AVM nidus. Angiography is still needed in the planning of either surgical or endovascular treatment of AVMs.

MR imaging and CT have nearly equal sensitivity for detecting angiographically evident intracranial arteriovenous malformations (AVMs) [1]. Optimal management of the patient with an AVM requires, however, more than just detection of the lesion. Elimination of the risk of intracranial hemorrhage is the primary indication for treatment in the majority of patients with AVMs. Since this can be guaranteed only if there is total resection or obliteration of the lesion, careful consideration must be given to the risks as compared with the benefits of any treatment. This assessment entails consideration of such factors as the size of the AVM nidus, the number and location of its feeding arteries, the characteristics of flow through the lesion, the degree of steal from normal brain parenchyma, and the pattern of venous drainage [2, 3]. Embolization of intracranial AVMs is of benefit in management, sometimes as a primary treatment method, but, more often, as an aid in reducing the operative risk. The purposes of this study were (1) to evaluate the utility of MR in assessing those factors known to be important in estimating the risk of surgical removal of AVMs and (2) to determine the capacity of MR to assess the effects of embolization of these lesions. The usefulness of MR in these assessments was compared with both conventional angiography and CT.

Materials and Methods

The MR images, CT scans, and angiograms of 15 consecutive patients with angiographically proved intracranial supratentorial AVMs were reviewed retrospectively. The nine men and six women (ages 16–68 years; median age, 35 years) who constituted this series presented with a variety of symptoms, the most common of which were chronic headaches ($n = 5$) and seizures ($n = 7$). Recent intracranial hemorrhage was the reason for evaluation in three patients; two others had a history of intracranial hemorrhage in the distant past (6 and 12 years ago, respectively). One had no symptoms related to his intracranial AVM but was examined because of a symptomatic spinal AVM.

This article appears in the March/April 1988 issue of *AJNR* and the May 1988 issue of *AJR*.

Received July 28, 1987; accepted after revision November 2, 1987.

Presented at the annual meeting of the American Society of Neuroradiology, New York, May 1987.

[1] Department of Radiology, University Hospital and Clinics, Madison, WI 53792. Address reprint requests to C. M. Strother.

[2] Present address: Department of Radiology, Rikshospitalet, N-0027, Oslo 1, Norway.

[3] Department of Neurosurgery, University Hospital and Clinics, Madison, WI 53792.

[4] Department of Radiology, Saint Marys Hospital, Madison, WI 53715.

[5] Department of Surgery, Dean Medical Center, Madison, WI 53715.

***AJNR* 9:225–235, March/April 1988**
0195–6108/88/0902–0225
© American Society of Neuroradiology

Biplane serial angiography and MR were performed in all 15 patients; 13 also had CT. Eight patients underwent embolization as part of their treatment; a variety of embolic agents (isobutyl 2-cyanoacrylate [IBC], polyvinyl alcohol sponge [PVA], glutaraldehyde cross-linked collagen [GAX], silastic spheres, and detachable balloons) were used. All of these patients had angiography, MR imaging, and CT both before and after embolization. Four patients in this series had resection of their AVM.

Angiography was performed with standard film-screen techniques as well as with intraarterial digital subtraction. In all instances, standard film-screen techniques were used for the initial angiographic evaluation; films were obtained using 2:1 geometric magnification, and the rate of filming was adjusted according to the speed of blood flow through the AVM.

MR was performed on a 1.5-T GE Signa unit. In all instances, images were obtained in at least two orthogonal planes; in nine instances, images in all three orthogonal planes were available. T1-weighted images were obtained using a TR of 350–800 msec and a TE of 20–30 msec. Proton-density and T2-weighted images were obtained using a TR of 2000 msec and TEs of 20–30 msec and 90–120 msec, respectively. The matrix size was 128 × 256 in eight patients and 256 × 256 in the other seven. Slice thickness ranged from 3–10 mm; the majority of studies were done using a 5-mm slice thickness.

CT was performed using third-generation scanners, either a GE CT/T 8800, a Siemens Somatom DR 3, or a Siemens Somatom DRH. Eleven patients were studied both with and without IV contrast, two were examined only without contrast. Only axial images were obtained; slice thickness varied between 4 and 10 mm.

Each of the three diagnostic techniques (MR, CT, and angiography) was evaluated separately to assess its utility in defining the size, characteristics, and location of the AVM nidus; its arterial supply and venous drainage; and the precise anatomic location of these structures. All studies were also evaluated for their ability to depict changes occurring after embolization. The ability of these techniques to detect associated parenchymal abnormalities, recent or remote hemorrhage, and the presence of mass effect was also determined. In an attempt to avoid bias, the MR images and CT scans were evaluated prior to assessment of the respective angiograms.

Results

Size of the AVM Nidus

In all of the AVMs a definite nidus—defined for purposes of this study as a tangle of more or less tightly packed abnormal vessels—was demonstrated by both angiography and MR. When using a 2:1 magnification correction factor for angiographic measurements, there was good correlation between the maximum diameters of the nidi as measured on corresponding angiograms and MR. Of the 11 patients who had a contrast-enhanced CT scan, measurements of the maximum nidus diameter made from CT and MR were in agreement in only three instances; in all of these, the maximum diameter of each nidus was oriented along the axial plane; that is, the plane of the CT scan. In six instances, CT measurements underestimated (0.5–2.5 cm) the maximum diameter of the nidus when these measurements were compared with those obtained with MR; in each of these, the maximum diameter of each nidus was oriented either along the sagittal or the coronal plane. In two patients the AVM nidus as seen on contrast-enhanced CT could not be separated from adjacent vascular structures, making measurement impossible. Measurement of nidus size could not be made in two instances in which only a noncontrast CT scan was available.

Arterial Feeders and Venous Drainage

All 15 AVMs in our series were predominantly pial; their arterial supply was derived from multiple arterial feeders (anterior cerebral artery) ($n = 10$), middle cerebral artery ($n = 12$), and the posterior cerebral artery ($n = 5$). One also had a significant dural component (middle meningeal artery). Although the proximal portions of the arterial feeders to these AVMs were clearly visualized with MR, angiography was superior to MR and CT for showing the details of the distal distribution of these vessels. The external carotid supply of the one AVM with a significant dural component was only identified with angiography.

Considering only the primary branches of the anterior, middle, and posterior cerebral arteries, there were, as determined by angiography, a total of 28 feeding arteries supplying the 15 AVMs; MR allowed unequivocal identification of 23 of these. Of those 11 AVMs studied with contrast-enhanced CT scans, 13 of 22 feeding arteries could be seen with this technique, while with MR 18 were identified.

A total of 45 draining veins (eight deep and 37 superficial), were identified angiographically in these 15 AVMs. Of these, 23 (seven deep and 16 superficial) were shown unequivocally by MR. In the 11 instances in which contrast-enhanced CT scans were available, CT demonstrated six of six deep-draining veins and 10 of 35 superficial ones; MR allowed detection of these same 16 veins as well as an additional four, all of which were superficial.

Precise Anatomic Location of the Lesion

Although angiography showed a larger number of feeding arteries and draining veins than either MR or CT, both MR and CT were superior to angiography in defining, once they had been identified, the precise relationships of these vessels to other structures. MR was, because of its multiplanar capabilities, better than CT in this regard (Fig. 1).

In all instances, both MR and CT were superior to angiography for demonstrating the precise anatomic location of the AVM nidi. Of the 11 patients with contrast-enhanced CT, MR and CT showed the location of the nidus equally well in two; in the remaining nine, MR contributed anatomic information not provided by CT. MR proved especially valuable for defining the location of the AVM nidi with respect to the surface of the brain, the ventricular system, and the corpus callosum (Figs. 2 and 3). A portion of the corpus callosum of three patients was replaced by the nidus; this finidng was shown only by MR (Fig. 3).

Detection of Recent and Remote Hemorrhage

Three patients were seen because of acute intracranial hemorrhage. Only CT scans were done in the acute phase of

Fig. 1.—Relationships between AVM nidus, arterial feeders, draining veins, and adjacent brain.

***A*, Coronal MR image (TR 600, TE 20) shows wedge-shaped nidus extending from cortex to ventricular surface. Within the nidus is a large draining vein. Enlarged arterial feeder is visualized in an adjacent sulcus. Note also visualization of lenticulostriate feeder.**

***B*, Posteroanterior angiogram of same patient. While vascular anatomy of this lesion is more clearly seen with this technique, its relationships to the brain are much more difficult to appreciate.**

***C*, Axial contrast-enhanced CT scan shows confluent contrast enhancement of AVM nidus. Arterial feeders and draining veins were not clearly distinguished with this technique.**

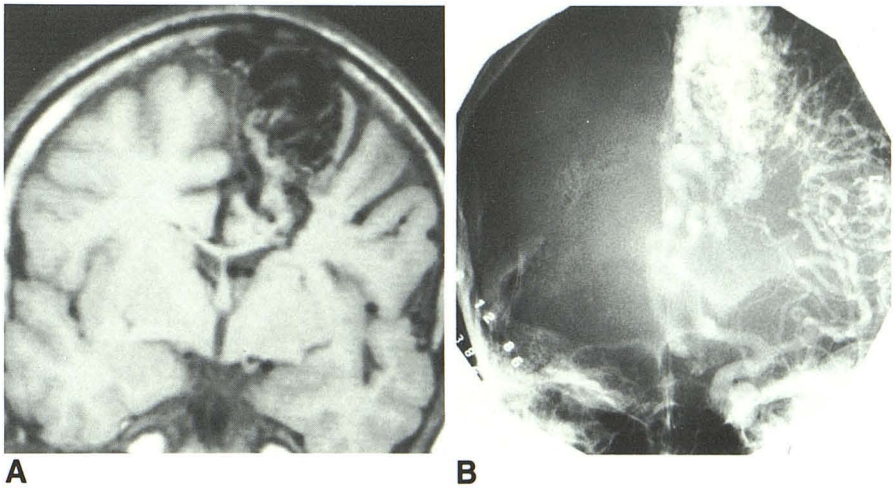

Fig. 2.—*A*, The exact relationships of this parasagittal AVM to the surface of the brain and the ventricle are clearly shown on this coronal MR image (TR 600, TE 20). Note involvement of left superior frontal gyrus with a thin rim of normal-appearing brain parenchyma lying both medially and laterally to nidus. Extension of nidus to the surface of ventricle is an important observation.

***B*, Posteroanterior angiogram shows AVM to be supplied by both anterior and middle cerebral feeders. Although these vascular features are clearly shown, the relationships of the nidus discussed above are much more obscure.**

their illness (less than 24 hr). In two, CT showed only intraventricular hemorrhage, while in the other, both a parenchymal and a subdural hematoma were demonstrated. Subarachnoid blood was not visualized with any technique in these three patients. An MR examination was performed on the patient who had both a parenchymal and subdural hematoma 3 days after the onset of his illness. Both these hematomas were seen as areas of high signal intensity on the T1-weighted images. T2-weighted images were not obtained. The presence of the parenchymal hemorrhage was demonstrated equally well on both CT and MR; its extent, however, could be more easily seen on MR than on CT (Fig. 4).

In the two patients with only intraventricular hemorrhage, the initial MR study was done 5 weeks and 8 months, respectively, after the acute bleed. The MR done 5 weeks after hemorrhage showed a persistent intraventricular hematoma; at this time intraventricular blood was no longer visible with CT (Fig. 5). Nine months later, evidence of this hemorrhage could no longer be seen with MR. The MR done 8 months after hemorrhage, documented with CT, demonstrated no sequela of this event; neither was there any sign of previous hemorrhage on CT scans done at this time.

MR showed evidence of old hemorrhage in only one of the two patients with a history of previous intracranial hemorrhage. In this patient, who had suffered an intracranial hemorrhage 12 years before the current studies, we found an area of high signal intensity on both T1- and T2-weighted images, surrounded by a rim of low signal intensity best seen

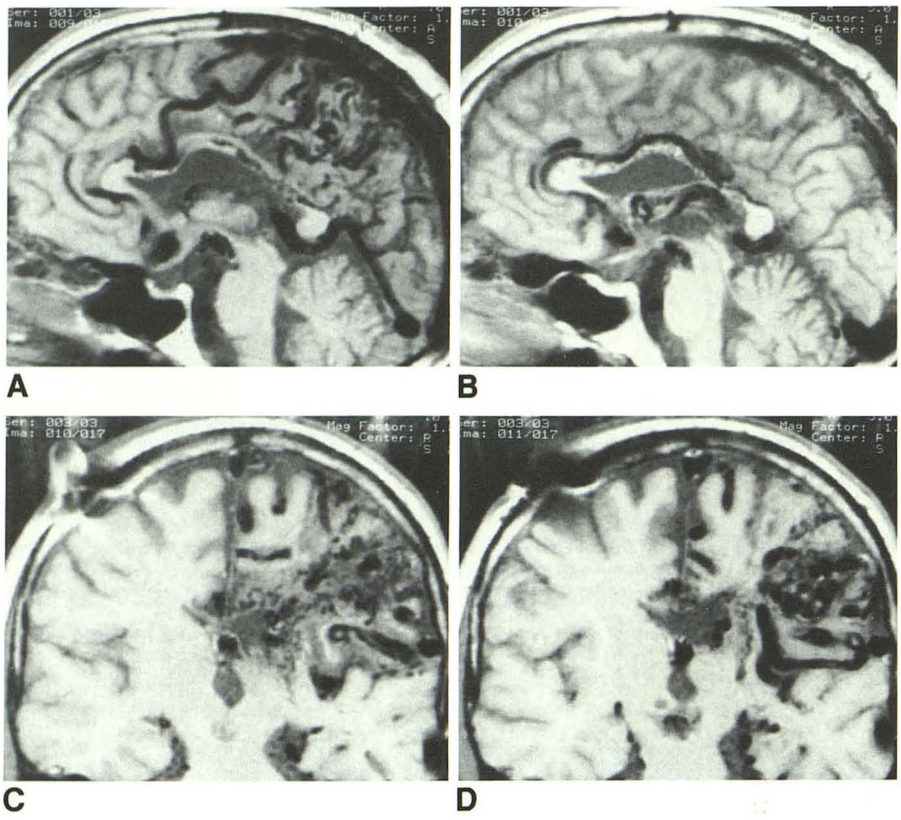

Fig. 3.—Replacement of part of corpus callosum by large left parietal AVM. Sagittal (*A* and *B*) and coronal (*C* and *D*) MR images (TR 600, TE 20). Note near total replacement by AVM of posterior half of the body of corpus callosum and marked thinning also of anterior half, which is penetrated by numerous small vessels. Large arterial feeders (anterior and middle cerebral) as well as large draining veins (internal cerebral and cortical) are also seen. The distortion and signal void in right parietal bone are due to a burr hole and a shunt.

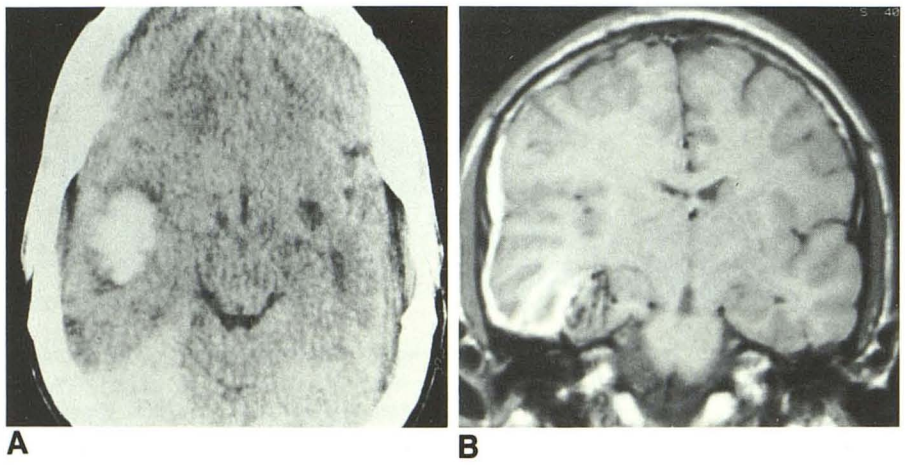

Fig. 4.—Right temporal lobe AVM with acute hemorrhage.

***A*, Noncontrast CT scan obtained shortly after hemorrhage shows left temporal lobe hematoma but no discernible extraaxial blood over lateral surface of hemisphere.**

***B*, Coronal MR image (TR 600, TE 20) obtained 3 days later. Part of AVM nidus and temporal lobe hematoma are seen. Note extracerebral hemorrhage extending along lateral surface of brain. Degree of mass effect shown on the two studies is similar.**

on T2-weighted images, thus indicating methemoglobin surrounded by hemosiderin [4] (Fig. 6). In the other patient, with CT documentation of an intracerebral and intraventricular hemorrhage 6 years before the MR study, we found no unequivocal evidence of previous hemorrhage. Specifically, neither methemoglobin nor hemosiderin could be identified by MR (Figs. 7 and 3).

Effect of AVM on Adjacent Brain Tissue

In the absence of evidence of an acute hemorrhage, mass effect from the nidus of an AVM was noted on the MR images of six patients. Evidence of equivalent mass effect was seen on CT scans in two of these, less mass effect than on MR in three, and no mass effect in the other. In no instance did CT show evidence of mass effect not seen on MR. Of the six patients shown to have mass effect, four had no associated venous varix.

In no patient were there, in the absence of definite clinical history of a previous hemorrhage, findings on either CT or MR of focal abnormality in the brain parenchyma surrounding an AVM nidus. In several patients there was, however, either unilateral or bilateral prominence of cortical sulci suggestive of atrophic changes. This alteration was more clearly seen on

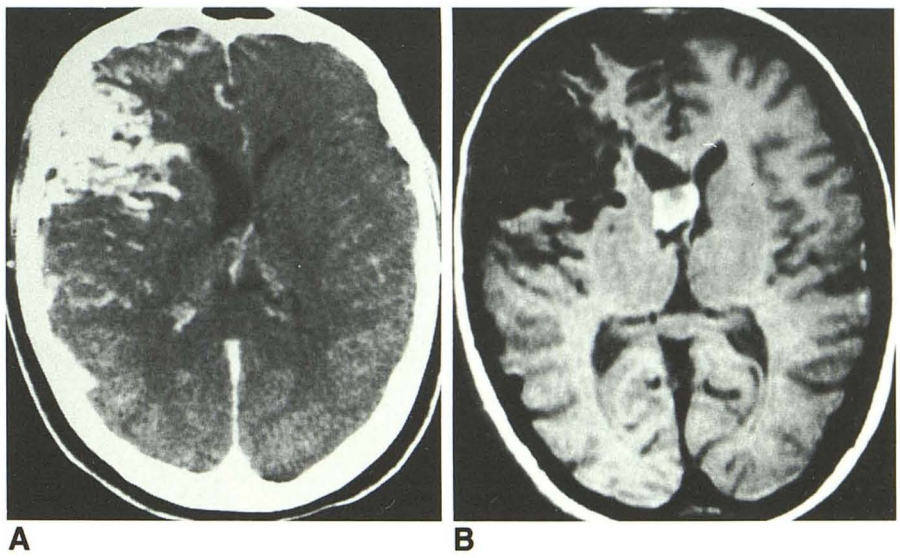

Fig. 5.—Intraventricular hematoma 5 weeks after hemorrhage.

***A*, Axial contrast-enhanced CT scan shows right frontal lobe AVM, dilated right lateral ventricle, and displacement of septum pellucidum toward the left. There is no direct visualization of any intraventricular hematoma.**

***B*, Axial MR image (TR 400, TE 20) through same level as in *A*. This study, obtained 2 days after the CT scan, demonstrates an intraventricular hematoma with high signal intensity due to presence of methemoglobin.**

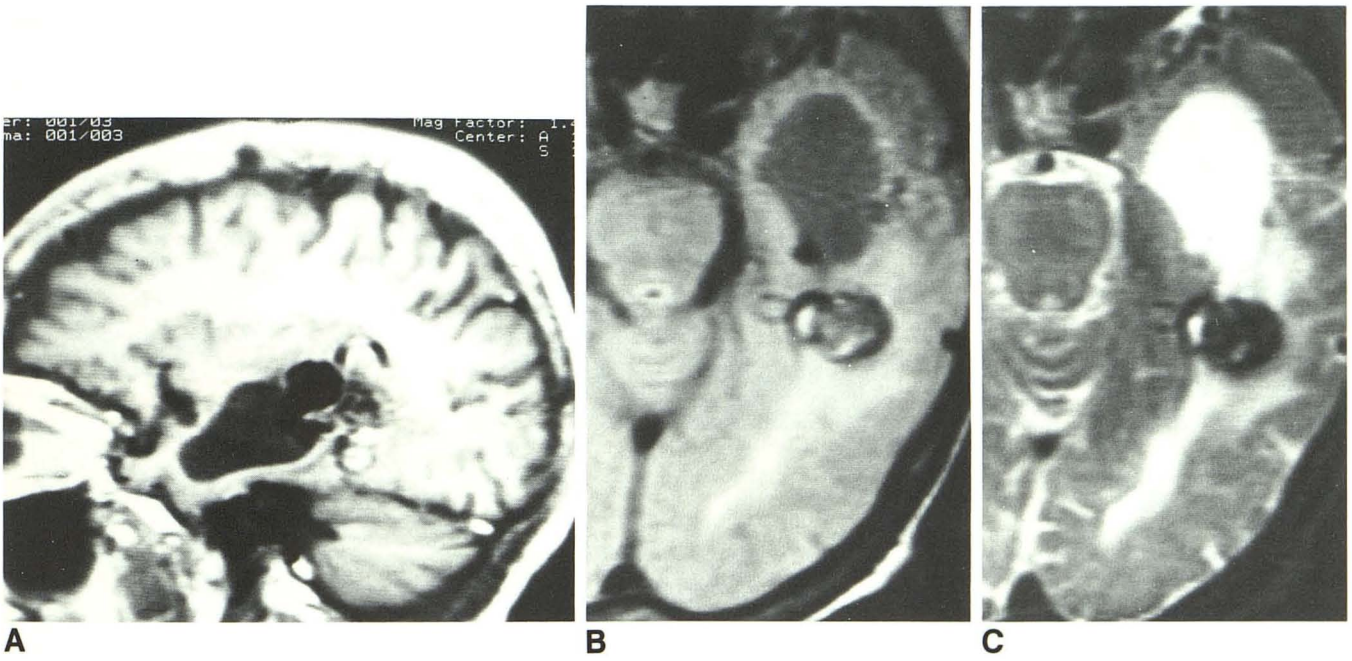

Fig. 6.—Left temporal lobe AVM with evidence of previous hemorrhage.

***A*, Sagittal T1-weighted MR image (TR 600, TE 30) shows area of high signal intensity just posterior to dilated temporal horn. A rim of low-signal-intensity tissue surrounds periphery of this lesion.**

***B* and *C*, Axial proton-density and T2-weighted MR image (TR 2000, TE 30 and 120) through same hematoma, which in this plane lies medial to a varix recently thrombosed as the result of embolization therapy. A small, peripheral, crescent-shaped area retains high signal intensity on heavily T2-weighted image, indicating methemoglobin; the lesion appears smaller than on proton-density image because of a more pronounced rim of low signal intensity, consistent with hemosiderin. High signal intensity is present in surrounding white matter. This may be the result of either ischemic change or more recent, unrecognized hemorrhage.**

MR. In two instances the segment of the corpus callosum that would be expected to transmit fibers originating from or entering into the brain parenchyma involved by an AVM nidus was hypoplastic (Fig. 8). These findings were only shown by MR.

Angiography was not of value in detecting the mass effect caused by these AVMs. It was the only technique, however, that provided direct evidence of arteriovenous shunting or of the presence of a steal phenomenon. Among the patients who demonstrated evidence of a vascular steal phenomenon by angiography, there was only one instance (Fig. 6) in which MR or CT showed any parenchymal abnormality (with the possible exception of prominent cortical sulci) that was suggestive of ischemia.

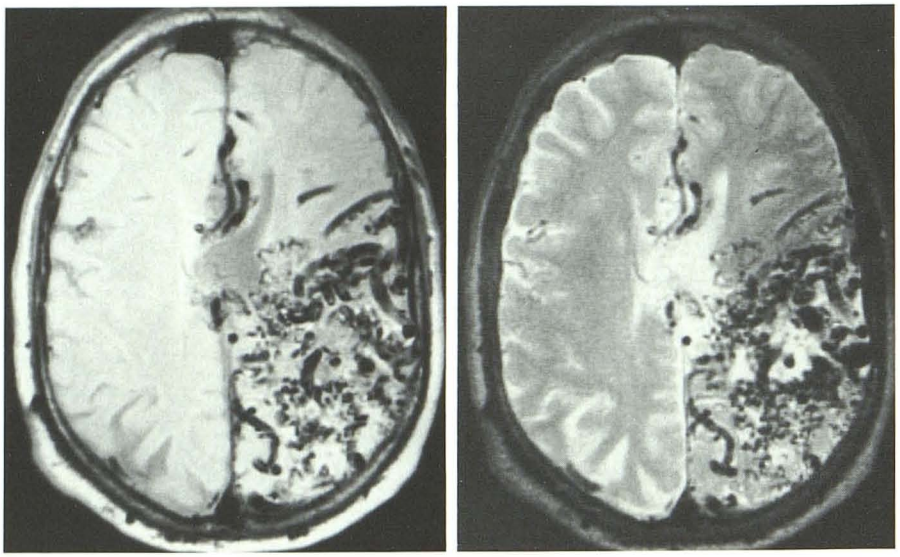

Fig. 7.—Axial MR image of large parietal lobe AVM that hemorrhaged 6 years earlier.

***A* and *B*, First-echo (*A*) (TR 2000, TE 20) and second-echo (*B*) (TR 2000, TE 90) MR images of multislice spin-echo sequence. Images fail to show unequivocal evidence of methemoglobin or hemosiderin. The area devoid of vessels in center of nidus is probably scarring (gliosis) due to previous hemorrhage; however, ischemic change cannot be excluded. A few very small bright areas seen on first-echo image in relation to vessels of nidus cannot be identified on second-echo image, and are probably due to flow-related enhancement. T1-weighted images of this AVM are shown in Fig. 3.**

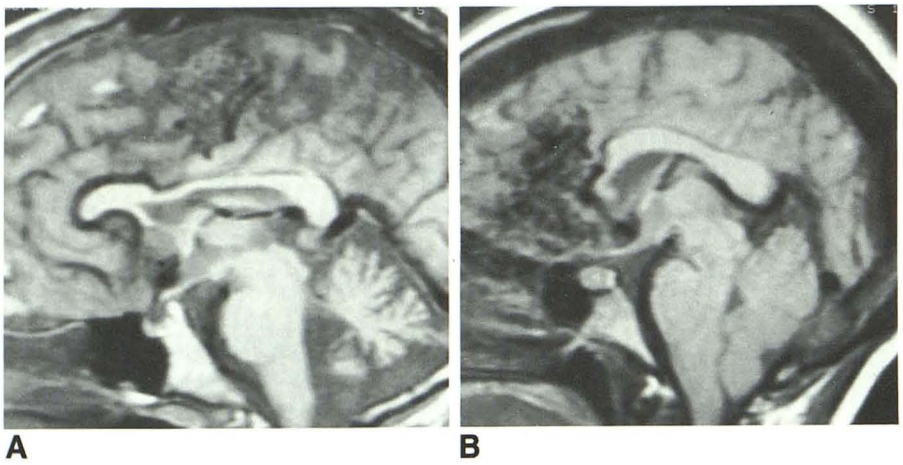

Fig. 8.—Hypoplastic changes of corpus callosum associated with an adjacent AVM.

***A*, Midsagittal MR image (TR 600, TE 25) shows thinning of body of corpus callosum in a patient with a large parasagittal AVM. The location and angiographic features of this lesion are shown in Fig. 2.**

***B*, Hypoplastic genu of corpus callosum in a patient with a large frontal lobe AVM. Midsagittal MR image (TR 400, TE 30). Note also enlargement of internal cerebral vein and vein of Galen resulting from deep venous drainage of this lesion.**

Effects of Endovascular Embolization

Eight of 15 patients were treated with endovascular embolization. In all, angiography was superior to both MR and CT in showing occlusions or diminished size of feeding arteries or draining veins after embolization.

CT was always superior to both angiography and MR in identifying and localizing the injected embolic material. With MR, embolic material mixed with water-soluble contrast medium could not be recognized. The only embolic agent shown by MR was IBC mixed with Pantopaque; this mixture had signal characteristics similar to those of fat, with high signal intensity on T1-weighted images and low signal intensity on heavily T2-weighted images. When IBC mixed with Pantopaque was dispersed throughout an AVM nidus, however, it was difficult to appreciate on MR images. In all cases it was easily detected on CT.

Compared with the other techniques, MR provided the clearest visualization of the internal features of the AVM nidi. Prior to embolization, the majority of the vessels constituting a nidus were seen as a tangle of round or oval-shaped structures having very low signal intensity on both T1- and T2-weighted images. Occasionally, a few of these vessels showed flow-related enhancement [1] (Fig. 7). Two types of nonvascular tissue were seen within the confines of many nidi. On T1-weighted images, the nonvascular interstices of nidi always had intermediate low signal intensity, similar to that of normal cortical gray matter (Fig. 9A). In some areas, this tissue remained of intermediate darkness on T2-weighted images, maintaining a signal intensity similar to that of normal white matter; in other areas, however, especially around the periphery of a nidus, it showed on these T2-weighted images a very high signal intensity, similar to that of CSF (Fig. 9B). Often, this high-signal-intensity tissue formed a distinct rim that extended around part of a nidus; sometimes it could be seen following along the course of large vessels entering or leaving a nidus. CT was not of use in assessing the internal characteristics of the AVM nidi.

In four of eight patients who were embolized, none of the three imaging techniques showed any definite changes within

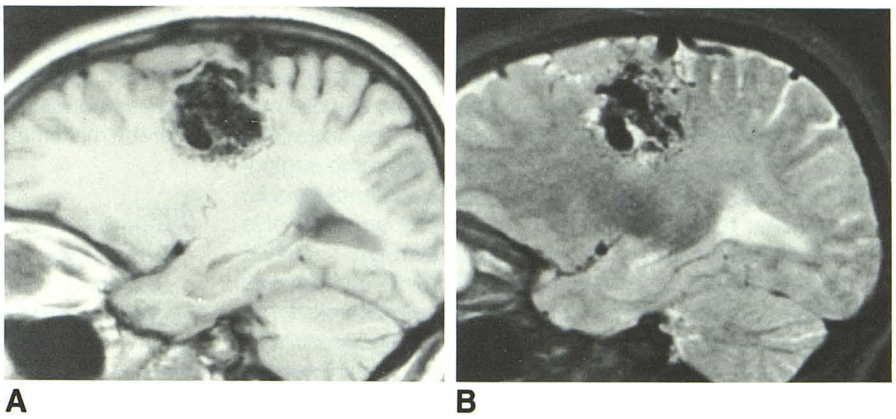

Fig. 9.—Signal characteristics of intervascular tissue in an AVM nidus.

A, Sagittal T1-weighted MR image (TR 600, TE 20) shows that tissue interposed between vascular components of nidus has intermediate low signal intensity.

B, T2-weighted MR image (TR 2000, TE 90) of same sagittal slice. Parts of intervascular tissue now have high signal intensity, similar to that of CSF; other parts have low signal intensity, similar to that of normal white matter.

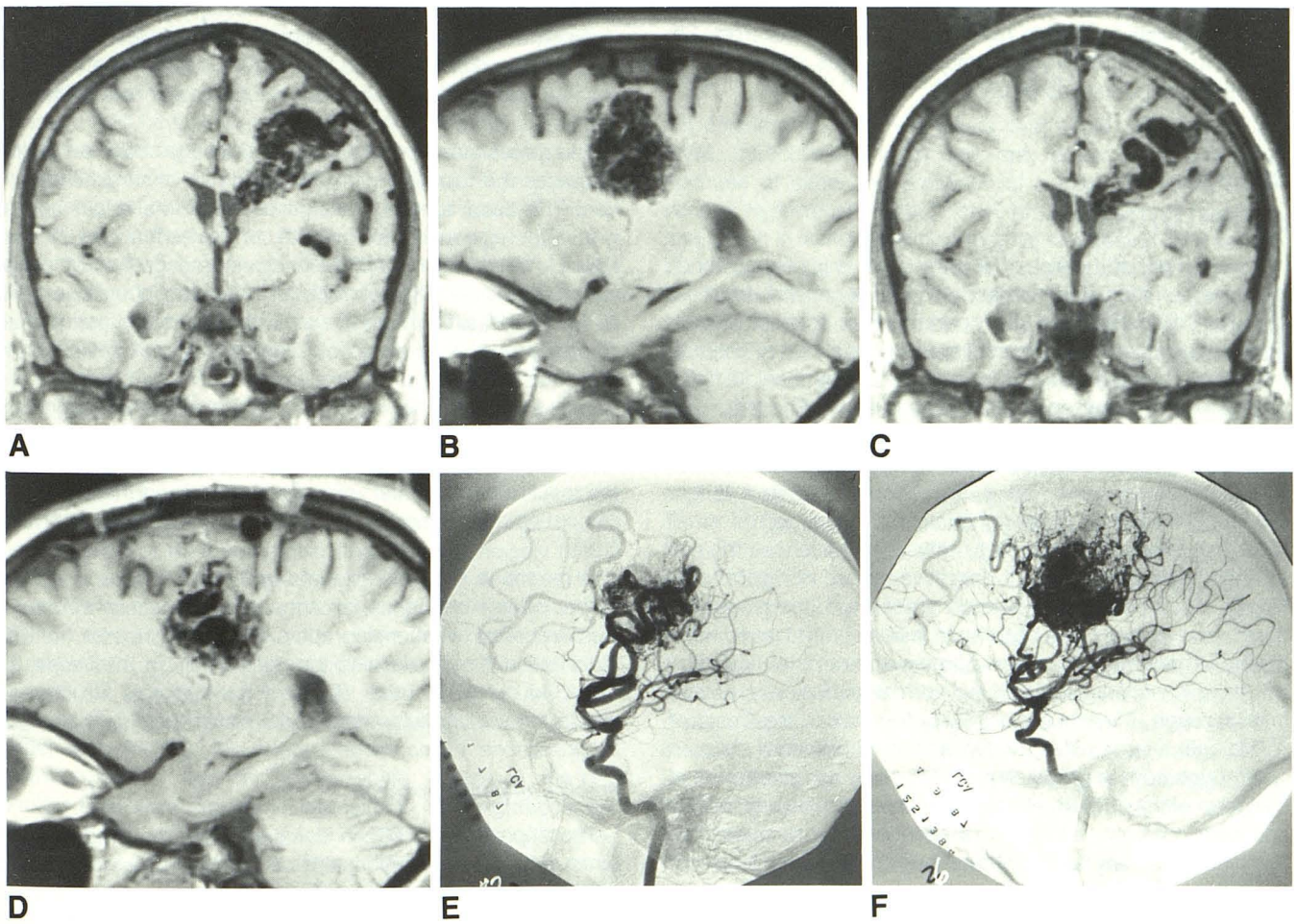

Fig. 10.—Effects of endovascular embolization.

A and *B*, Preembolization coronal and sagittal MR images (TR 600, TE 20) show large wedge-shaped AVM extending from cortex of frontal lobe to angle of frontal horn.

C and *D*, Coronal and sagittal MR images at same location as those in *A* and *B*, done after four embolizations with polyvinyl alcohol (PVA). There has been a dramatic change in signal intensity with nidus, areas of flow void being replaced by tissue with isointense signal characteristics. This is believed to represent obliteration of nidus. The least change is seen at apex of nidus, an area supplied by lenticulostriate arteries that were not embolized. Note reduction in size of middle cerebral artery feeders deep within sylvian fissure. There is no change in size of large draining vein. The small extracerebral collection is the sequela of one intraoperative embolization (anterior cerebral artery).

E and *F*, Pre- and postembolization angiograms for comparison. Although alteration in size of feeding arteries that were embolized is evident, it is more difficult to detect alterations within nidus itself.

the nidus. In the other four, varying degrees of decreased opacification of the nidus were seen at angiography. CT proved of little value for detecting changes within the nidus of an embolized AVM, since enhancing vessels, embolic material, and calcification could not be separated from one another in the same image. MR was superior to both angiography and CT in showing occlusion of vessels in the nidus, and was the technique that best defined those parts of a nidus in which blood flow had been obliterated.

After embolization, cessation of blood flow in a nidus was recognized on MR images by the lack of signal void in an area where flow void had previously been seen. Areas of a nidus that prior to embolization had very low signal intensity were transformed after embolization into homogeneous gray areas on both T1- and T2-weighted images (Fig. 10). Embolized vessels within a nidus without flow void were indiscernible from the intermediate-dark signal intensity nonvascular tissue with all pulse sequences used. Except for those cases embolized with an IBC/Pantopaque mixture, high signal intensity in the embolized portion of a nidus was not observed with any pulse sequence over a follow-up period from 1½ weeks to 6 months. No postembolic changes were found in the nonvascular tissues of the nidi.

Discussion

Size of AVM Nidus

Assessment of the size of an AVM's nidus is of importance because as nidus size increases so do, in general, both the technical difficulties and the operative risk associated with surgical resection. Recent grading systems aimed at estimating the risk associated with surgical therapy include nidus size as one of the attendant risk factors [2, 3]. The larger the size of an AVM nidus, the greater the amount of normal brain parenchyma that must be exposed for operative removal. Resection of an AVM with a large nidus requires a longer operating time than does removal of a lesion with a small nidus in a similar location; thus, nidus size influences the risk of anesthesia as well as of operative-related complications. Finally, nidus size bears some correlation with the amount of blood flow through an AVM; those lesions with a large nidus having in general both larger volumes and rates of flow than do lesions with a small nidus. Normal perfusion pressure breakthrough [5] is thus more likely to occur in treatment of AVMs with a large nidus than in lesions with a small nidus.

Although both angiography and CT allow demonstration of the nidus of an AVM, the multiplanar tomographic capabilities and high contrast resolution of MR combine to make this technique superior to the others in showing the full size of the nidus. In our series, CT underestimated the size of an AVM nidus in six cases; these were all due to the single-plane imaging technique used, and probably occurred as a result of partial volume averaging. As in the axial projection, the full extent of the lesion in the craniocaudal direction could not be demarcated from adjacent brain and normal vasculature. In two other patients, it was impossible to define clear borders of the AVM nidus on the CT images. On contrast-enhanced scans, enhancement of these AVMs appeared homogeneous. Such a confluent pattern makes identification of individual vessels impossible; the adjacent draining veins and feeding arteries on such images blend imperceptibly with the nidus, thereby making exact measurement impossible.

Arterial Suppy and Venous Drainage

In our study, angiography was superior to both CT and MR as a technique for showing the feeding arteries and draining veins of an AVM. A major reason for this advantage was that the 5–10-mm slice thickness used for both the CT and MR studies rendered invisible, because of partial volume averaging, the majority of feeding arteries and draining veins. The capability of obtaining 3-mm slices was available for only one of our patients. In this instance, MR clearly showed even small feeding arteries such as a lenticulostriate artery. Even though partial volume averaging effects can be minimized through the use of thin sections, intrinsic to the tomographic images of both CT and MR is the difficulty of providing a clear three-dimensional impression of tortuous vessels. Angiography was the only technique that allowed recognition of those lesions with rapid arteriovenous shunting and arteriovenous fistulae.

The presence of deep venous drainage from an AVM increases the technical difficulties and risk of surgical resection. The deep venous drainage of the AVMs in our series was detected equally well by both contrast-enhanced CT and MR. However, with both techniques, recognition of deep venous drainage is dependent on a substantial enlargement of the deep draining vein(s), and when such veins are normal or nearly normal in size, only angiography will reveal their presence.

Both CT and MR were less accurate in allowing recognition of the superficial venous drainage from an AVM than they were in detecting deep venous drainage. This deficiency is the result of both partial volume averaging and the presence of normal large vascular structures over the surface of the brain.

In regard to both the arterial supply and venous drainage of the AVMs in our series, once a particular vascular structure was identified with angiography, MR was superior to the other techniques in defining the relationship of the vessel to the AVM nidus, to other adjacent parenchymal structures, and to the ventricular system and subarachnoid space.

Precise Anatomic Location

The superiority of MR in demonstrating the precise anatomic location and relationships of an AVM nidus, its feeding arteries, and draining veins is probably the most important advantage offered over CT and angiography. The highly detailed anatomic information provided by MR and its presentation in the sagittal, coronal, and axial planes provides the neurosurgeon and interventional neuroradiologist with unique information for planning treatment. At the surface of the brain, the exact relationships between the nidus, individual gyri, and overlying vascular structures can be shown; deep compo-

nents of a lesion can be located precisely with respect to the ventricular system, corpus callosum, and basal ganglia. Precise anatomic localization of this nature should also prove to be of value in planning radiation therapy of AVMs.

Detection of Recent and Remote Hemorrhage

The usefulness of MR in detecting intracranial hemorrhage is well established [4, 6, 7, 8]. Acute hemorrhage from an AVM is easily detected by CT, but may be more difficult to diagnose with MR, especially when imaging is done at lower field strengths [9]. In our study, no acute hemorrhage was studied with MR, the earliest MR images being obtained 3 days after clinical and CT evidence of a hemorrhage. In this case, both a subdural and parenchymal hemorrhage had a high signal intensity on T1-weighted images, indicating the presence of methemoglobin. The duration that methemoglobin persists within a hematoma is variable; however, intracerebral hematomas may contain methemoglobin for at least several months [10]. In one of our patients, methemoglobin was present within an intraventricular blood clot 5 weeks after its occurrence. In another of our patients, tissue with signal characteristics typical for methemoglobin was seen 12 years after a known hemorrhage. Because some hemorrhages from AVMs are clinically silent [11], the small hematoma seen in this patient could have been of more recent origin. Definite evidence of an old hematoma was thus found with MR in only one of two patients that had a clinical history of remote hemorrhage and in none of 10 patients without prior clinical history of hemorrhage. Microscopic foci of hemosiderin-laden macrophages are almost always present within the nidus of an AVM [12], thus indicating that clinically occult hemorrhages are common in AVMs. The reasons for our inability to detect these hemorrhages with MR in the majority of our patients are several. Areas of high signal intensity within an AVM nidus may be due to either flow-related enhancement [1] or methemoglobin. Usually this distinction can be made if images from different pulse sequences are compared. Furthermore, the presence of methemoglobin does not necessarily result in high signal intensity. Methemoglobin has a structure that allows water molecules to approach its paramagnetic center wtihin a few angstroms, thereby promoting dipole-dipole or T1 relaxation [13]. This dipole-dipole interaction increases the T1 and T2 relaxation rates (1/T1 and 1/T2) equally, but because the T1 of blood (as well as other tissues) is much longer than the T2, the relative effect on T1 shortening is much larger than that on T2 shortening. Therefore, the net result is typically a high signal intensity on T1-weighted (short TR, short TE) images. Very high concentrations of methemoglobin could, however, lead to a T2 shortening of such a degree that the area would appear either isointense or hypointense to brain parenchyma on both T1- and T2-weighted images. At least theoretically, this could explain the lack of detectable methemoglobin in some of our patients.

Over time, however, all methemoglobin is resorbed and only hemosiderin within macrophages remains (perhaps forever) as evidence of a previous hemorrhage. Hemosiderin promotes preferential T2 shortening. Its presence can be recognized by an area of low signal intensity, most pronounced at high field strengths and on heavily T2-weighted images [4]. Although these appearances are in some ways similar to those of calcifications, it should be possible to distinguish the two, as the signal intensity from most pathologic parenchymal calcifications is normally somewhat greater than that resulting from depositions of hemosiderin. Additionally, the signal intensity from an area of calcification does not decrease with increases in TE to the same extent as does that from an area of hemosiderin deposition. The detection of previous hemorrhage associated with an AVM may be of importance in that such a finding has been considered to indicate increased risk of subsequent hemorrhage [11]. Our study indicates, however, that the sensitivity of high-field-strength MR in detecting hemosiderin within an AVM nidus is relatively low. The foci of hemosiderin-laden macrophages commonly found histologically may have a size below the spatial resolution of MR, and, of equal importance, even if seen, may be impossible to separate from the numerous low-signal-intensity vessels of the nidus.

Effect of AVM on Adjacent Brain Tissue

Considerable evidence exists that brain adjacent to an AVM, particularly a large one, may suffer adverse effects because of either the presence of a steal phenomenon or venous hypertension [14]. Either of these two mechanisms may result in ischemia, which may be manifested by a variety of neurologic signs or symptoms, including seizure disorders. MR has been shown to be more sensitive than CT in detecting ischemic changes in brain; and, in a recent report, apparent ischemia in brain adjacent to an AVM was demonstrated with MR [15]. In our series, no MR evidence of steal (i.e., ischemia) was found. The white-matter changes seen in one patient who also had evidence of a remote hemorrhage were probably not the result of edema but rather a manifestation of leukoencephalomalacia due to the previous hemorrhage. However, of our 15 patients, 10 showed angiographic signs of a steal. Five of these 10 had a seizure disorder and three had a global deterioration in their neurologic function, without specific localizing signs or symptoms. In this group, the lack of findings in the brain adjacent to the AVM illustrates the inability of MR, as it was performed on our patients, to demonstrate ischemic change prior to a point when significant edema or cell damage occurs. Proton MR thus appears to be rather a crude tool for measuring cerebral hypoperfusion. The steal phenomenon seen with angiography reflects only changes occurring in the input vessels of the brain and lacks direct correlation with the functional status of the patient.

In our study, the effects of AVMs on adjacent brain tissue were those of mass effect and interruption of axonal pathways. Although generally AVMs tend to replace brain tissue and do not, in the absence of hemorrhage, act as mass lesions, many exceptions occur. This finding has been described by Viñuela et al. [16] and is further illustrated by our study. The better detection of mass effect with MR than with CT reflects simply the superiority of multiplanar over uniplanar imaging. The clinical significance of mass effect caused by an

AVM that has not hemorrhaged is not known. It seems reasonable, however, that mass effect can play a contributory role in causing functional derangement of adjacent brain parenchyma, and thus its recognition is of potential importance in managing this group of patients.

The magnitude of a deficiency of neural parenchyma resulting from the presence of an AVM is difficult to appreciate either on CT scans or with angiography. In two of our patients, each of whom had a large parasagittal AVM, focal thinning in the body of the corpus callosum was found to correspond in location to that of the expected position of fibers having as their origin or destination the portion of the brain that was replaced by the AVM nidus. Presumably, these AVMs were responsible for these changes. Such detailed anatomic information was only available by direct inspection prior to the availability of MR, and to our knowledge has not been previously reported. Although such observations do not provide information that is of immediate therapeutic consequence, they do offer some insight into the origin of some of the poorly defined neurologic manifestations of cerebral AVMs.

Effect of Endovascular Embolization

The ideal goal of embolization therapy of an AVM is obliteration of its nidus. Complete elimination of the nidus is curative, but is seldom achieved by embolization alone. More often, embolization is helpful as a preoperative procedure, either by conversion of an inoperable lesion into one that can be removed or as a means to eliminate a portion or portions of the nidus, which, because of their location or blood supply, make them difficult to deal with surgically.

In the majority of instances, assessment of the effects of embolization of an AVM is quite imprecise. This is the result of the modular architecture of these lesions, the persistence of enlarged draining veins until the arterial input has been eliminated, and perhaps of most importance, the inability, prior to availability of MR, to visualize clearly changes that occur within the nidus itself. Although angiography provides clear delineatiion of postembolization alterations that occur in the feeding arteries of an AVM, it is difficult, using angiography, to be certain about the validity of changes seeming to occur in the nidus. Alterations in the extent and rate of nidus opacification as well as in its size may occur secondary to a variety of causes. Important among these are variations in the volume and rate of contrast medium injected, variations in the placement of the catheter tip, arterial spasm, and hemodynamic changes that occur as a result of variation in heart rate, blood pressure, or arterial blood-gas concentrations.

As compared with both CT and angiography, MR provided the clearest visualization of the internal architecture of the nidi of the AVMs in our series. The multiplanar, tomographic capabilities and high contrast sensitivity of MR account for this superiority. Only MR allowed definition of the nonvascular components of an AVM nidus.

Alterations in the MR signal produced by blood flow (i.e., the conversion of an area within a nidus from one that showed significant flow void to one with a lack of flow void), or in other signals indicating flow, seemed to be the most reliable and sensitive way of demonstrating alterations occurring within the nidus after embolization. The lack of an MR signal from an area of calcification could, in theory at least, cause difficulty in differentiating the pathologic calcifications that are frequently present within an AVM from vessels having rapidly flowing blood, and thereby limit the usefulness of the technique for detecting changes in the nidus after embolization. In our experience, such areas of calcification usually have slightly higher signal intensity than do vascular structures that contain rapidly flowing blood; probably because the small and irregular configuration of the calcifications make partial volume averaging of signal likely. The irregular shape of most such calcifications aids further in their distinction from vascular structures, which, as a rule, tend to be quite regular.

Unlike CT, in our study, MR proved to be of little or no value for identifying the presence of embolic material within an AVM. Although visualization of embolic material is of some interest, the failure to do so with MR does not represent a significant limitation in the use of this technique for assessing changes occurring after embolization. The mere presence and amount of embolic agent within an AVM does not relate directly to the effectiveness of embolotherapy (i.e., to the degree of nidus obliteration).

Conclusions

We believe MR to be superior to both CT and angiography as a technique for determining the size and location of an AVM nidus, for detecting the effects of an AVM on adjacent brain, and for showing the extent of AVM nidus obliteration after embolization. MR is more sensitive than CT for detecting subacute and old hemorrhage, but because of flow-related artifacts and low sensitivity in distinguishing calcifications from rapid flow and/or hemosiderin it seems to have a low sensitivity for detecting remote hemorrhages within an AVM nidus. Although angiography is seldom needed as a tool for the diagnosis of an intracranial AVM, it remains the only technique that can provide the detailed vascular and hemodynamic information needed to plan either surgical or endovascular treatment of these lesions. The single most important advantage of MR is its ability to precisely define the relationship of the AVM to the adjacent brain surface, the ventricular system, and the feeding arteries and draining veins. MR should play a key role in the management of patients with supratentorial AVMs.

REFERENCES

1. Bradley WG. Magnetic resonance appearance of flowing blood and cerebrospinal fluid. In: Brant-Zawadzki M, Norman D, eds. *Magnetic resonance imaging of the central nervous system.* New York: Raven, **1987**:83–93
2. Shi YQ, Chen XC. A proposed scheme for grading intracranial arteriovenous malformations. *J Neurosurg* **1986**;65:484–489
3. Spetzler RF, Martin NA. A proposed grading system for arteriovenous malformations. *J Neurosurg* **1986**;65:476–483
4. Gomori JM, Grossman RI, Goldberg HI, et al. Intracranial hematomas: imaging by high-field MR. *Radiology* **1985**;157:87–93
5. Spetzler RF, Wilson CB, Weinstein P, et al. Normal perfusion pressure

breakthrough theory. *Clin Neurosurg* **1978**;25:651–672
6. Bradley WG, Schmidt PG. Effect of methemoglobin formation on the MR appearance of subarachnoid hemorrhage. *Radiology* **1985**;156:99–103
7. Kucharczyk W, Lemme-Pleghos L, Uske A, et al. Intracranial vascular malformations: MR and CT imaging. *Radiology* **1985**;156:383–389
8. New PFJ, Ojemann RG, Davis KR, et al. MR and CT of occult vascular malformations of the brain. *AJNR* **1986**;7:771–779
9. Sipponen JT, Sepponen RE, Sivula A. Nuclear magnetic resonance (NMR) imaging of intracerebral hemorrhage in the acute and resolving phases. *J Comput Assist Tomogr* **1983**;7:954–959
10. DiChiro G, Brooks RA, Girton ME, et al. Sequential MR studies of intracerebral hematomas in monkeys. *AJNR* **1986**;7:193–199
11. Luessenhop AJ. Natural history of cerebral arteriovenous malformations. In: Wilson CB, Stein BM, eds. *Intracranial arteriovenous malformations*. Baltimore: Williams & Wilkins, **1984**:12–23
12. McCormick WF. Pathology of vascular malformations of the brain. In: Wilson CB, Stein BM, eds. *Intracranial arteriovenous malformations*. Baltimore: Williams & Wilkins, **1984**:44–63
13. Eisenstadt M. NMR relaxation of protein and water protons in methemoglobin solutions. *Biophys J* **1981**;33:469–474
14. Spetzler RF, Selman WR. Pathophysiology of cerebral ischemia accompanying arteriovenous malformations. In: Wilson CB, Stein BM, eds. *Intracranial arteriovenous malformations*. Baltimore: Williams & Wilkins, **1984**:24–31
15. Bradley WG. Pathophysiologic correlates of signal alterations. In: Brant-Zawadzki M, Norman D, eds. Magnetic resonance imaging of the central nervous system. New York: Raven, **1987**:23–42
16. Viñuela FV, Fox AJ, Pelz DM, Drake CG. Mass effect of giant intracerebral varices secondary to high-flow AV fistulae: unusual cases in children and adults. *AJNR* **1984**;5:673 (abstr)